Self-Supervised Segmentation of River Scenes

Supreeth Achar, Bharath Sankaran, Stephen Nuske, Sebastian Scherer and Sanjiv Singh.

***Abstract*— Here we consider the problem of automatically segmenting images taken from a boat or low-flying aircraft. Such a capability is important for autonomous river following and mapping. The need for accurate segmentation in a wide variety of riverine environments challenges the state of the art vision-based methods that have been used in more structured environments such as roads and highways. Apart from the lack of structure, the principal difficulty is the large spatial and temporal variations in the appearance of water in the presence of nearby vegetation and with reflections from the sky. We propose a self-supervised method to segment images into 'sky', 'river' and 'shore' (vegetation + structures) regions. Our approach uses assumptions about river scene structure to learn appearance models based on features like color, texture and image location which are used to segment the image. We validated our algorithm by testing on four datasets captured under varying conditions on different rivers. Our self-supervised algorithm had higher accuracy rates than a supervised alternative, often significantly more accurate, and does not need to be retrained to work under different conditions.**

I. Introduction

We are interested in a minimal sensor suite based on passive vision and inertial sensing that could be used to autonomously explore rivers, mapping their width as it proceeds. Given sensor pose and camera calibration segmented images can be turned into river maps. In some cases, the canopy can be so thick and high around a river so as to block GPS signals and the problem becomes one of simultaneous localization and mapping. In this paper, we focus on the key subproblem of automatically segmenting images so that the extents of the river can be found accurately. Since rivers can look like roads, one idea is to use fairly well developed methods that have been used to track roads and highways with passive vision. Apart from the lack of structure such as clearly defined road edges, the principal difficultly of vision-based tracking of rivers has to do with large spatial and temporal variations in appearance of water in the presence of nearby vegetation and with reflections from the sky. See for example, Fig. 1 and Fig. 2.

Such problems are often solved with supervised learning, an approach where a system is trained based on representative data ahead of time. In our case, supervised learning would require that we train our river detector with instances of image regions that correspond to water in rivers and then use the trained system online. Given the lack of a representation that would render the appearance of rivers as a constant under varying conditions, we find that it is necessary that any learning be self-supervised. That is, the system must train itself, adapting to local appearance as influenced by terrain, flora and lighting conditions. A natural question arises in being able to develop such a self-supervised method– whence the representation? There is a common intuition that features of color, texture and vertical location in an image might help. Still, at the outset it is not clear how to encode/combine different features.

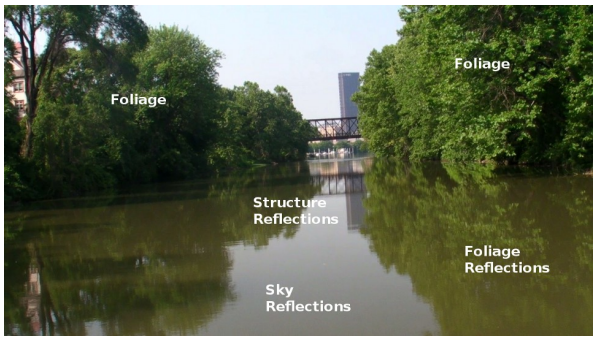

Fig. 1. An example image illustrating the variation of river appearance within a single image.

Here we propose a two step self-supervised method to perform such segmentation. In the first step we use a simple heuristic (knowledge of the horizon line) to automatically determine the relative correlation between features (a grab bag of color and texture based features). This allows us to score each image patch on its likelihood of belonging to a river. Patches with high confidence labels are used to train a Support Vector Machine. In the second step, the output of the SVM segments the image into distinct regions. The

Fig. 2. This image was taken from almost the same location as Fig. 1 at a different time of day. The appearance of the river has changed dramatically.

S. Achar, S. Nuske, S. Scherer and S. Singh are with The Robotics Institute, Carnegie Mellon University, Pittsburgh, PA 15232, U.S.A., {supreeth,nuske,basti,ssingh}@cmu.edu

B. Sankaran is with the GRASP Laboratory, University of Pennsylvania, Philadelphia, PA, 19104, U.S.A, bharath@seas.upenn.edu

advantage of such an approach is that it assumes no prior to determine segmentation other than simple geometric assumptions such as that the river lies below the horizon, and, that river features are significantly different than other features below the horizon. All other training happens automatically as often as at every frame.

We have tested our algorithms with image sequences from two different rivers, the image sequences have different environmental conditions; sunny and dusk, summer and fall. We show how supervised learning by training with hand labeled instances of segmentation, provides a reasonable solution but does not generalize well to novel environments. We show how performance and adaptability to novel environments can be improved with a self-supervised algorithm.

II. Related Work

Work related to the river segmentation algorithm presented in this paper falls into three main categories: techniques for inferring geometry from appearance, road following methods and water hazard detection systems for autonomous ground vehicles.

Make3D [1] and Photo Popup [2] infer information about scene structure from appearance. These methods work well on a wide variety of images but tend to have problems dealing with reflections and shadows which are common in riverine environments. Also, both these methods are computationally intensive which precludes their use in time sensitive applications.

Our work is similar in purpose to road following algorithms. In [3] a self-supervised road segmentation algorithm was proposed that used a laser scanner to find a small region of road directly in front of the vehicle which was used to build a road appearance model and classify the rest of the image. The underlying assumption is that road appearance is fairly uniform, but as is clear in Fig. 1 river appearance is inhomogeneous so an appearance model learnt on a small patch near the bottom of an image would not be representative of appearance of the entire river region.

There has also been work in detecting water hazards for autonomous ground vehicles. Approaches have been proposed based on polarized imagery [4], [5] and hyperspectral imaging [6]. For reasons of cost and weight restrictions we consider a visible light camera solution.

In [7] and [8] water is detected in stereo imagery by fusing color, brightness and stereo disparity cues with a rule based classifier. Recently in [9], the same authors used a physical model of water reflectance to detect water bodies in monocular images. They make the observation that in their application environment the color of a water body gradually changes from the leading edge to the trailing edge (as a function of incident angle), while other terrain types do not. They use this observation to detect water bodies in wide-open areas. Riverine environments are not wide open and variation in river appearance is more dependent on the reflections of the surrounding environment than on incident angle.

Rather than learn or derive a model offline of how the river will appear, we take an online approach that assumes a ground plane (river plane) and exploits the knowledge of the horizon to create self-supervised training sets from the current image.

III. Feature Selection

To enable effective river segmentation a discriminative feature vector ($X \in \mathbb{R}^d$) for describing local appearance is required. Color is a useful feature for detecting water as demonstrated in [7] & [8]. Texture is another useful cue, for example, parts of an image containing the river tend to be less textured than regions of foliage. Position in an image provides a strong prior, the higher up in an image a region is the less likely it is to be part of the river.

We selected features by empirically measuring the performance of different feature vectors describing color and texture in a supervised learning setup. Each candidate feature vector was used to train a two class (river and shoreline) linear support vector machine over a set of training images and then tested by using the SVM to segment the river in images from a small evaluation dataset. Performance of a feature vector was quantified by the percentage of correctly labeled pixels averaged over the evaluation dataset. All features were calculated over 5×5 pixel patches.

To choose a color descriptor for the feature vector we used the RGB, Lab and HSV color spaces individually and in various combinations to train classifiers. The performance of these classifiers on labeling river regions in the evaluation dataset is show in Table I. A combination of RGB and Lab colorspaces gave the best performance and was selected as our color descriptor. Although both RGB and Lab encode the same color information, combining them allows a linear classifier to learn a more complex decision boundary.

We evaluated the performance of three texture descriptors using a similar methodology. The first was the response to a set of Laws' masks [10]. We used 8 of the 9 3×3 Laws' Masks leaving out the mask that performs low pass filtering. Responses to each of these filters was calculated over 4 scales on the 3 channels of the Lab image, so the resulting texture descriptor had length $4 \times 3 \times 8 = 96$. The second texture descriptor considered was the unnormalized DAISY descriptor [11]. The third alternative was a bank of Gabor filters with 4 scales and 6 orientations. For all the texture descriptors, filter responses were normalized with respect to intensity. All three filter sets performed almost equally (Table I) so we chose the Laws' masks because it was the fastest to compute.

When combined, color and texture features perform better than either cue alone. Image position, specifically the height of a region in image coordinates, provides a strong contextual cue for segmentation and is included in the feature vector. The bottom of Table I shows the labeling error rate for the combined color and texture descriptor and for our final choice of feature descriptor with a fully supervised classifier on the images in the evaluation dataset.

IV. Self-Supervised River Segmentation

Riverine environments vary widely in appearance which makes building a single classifier that works well in different

TABLE I

PERFORMANCE OF DIFFERENT FEATURE VECTORS FOR SEGMENTATION INTO TWO CLASSES

	Feature	Dimensionality	Error Rate
Color	RGB	3	47.05%
	Lab	3	35.61%
	HSV	3	46.62%
	RGB+HSV	6	44.43%
	RGB+Lab	**6**	**32.90%**
	RGB+Lab+HSV	9	37.60%
Texture	**Laws' Masks**	**96**	**26.81%**
	DAISY	200	26.76%
	Gabor	24	27.19%
Combined	Color+Texture	102	19.73%
	Color+Texture+Height	**103**	**4.61%**

conditions difficult. Such a classifier would require labeled training images captured in many environments under different conditions. Its performance in an environment dissimilar to those seen earlier would not be assured. Instead of attempting to learn offline a universal model of river appearance, we automatically learn a new appearance model online for each new input image.

To do this we utilize knowledge about the position of the horizon in each image and assume that anything appearing above the horizon line is not part of the river. The assumption that the river can not be above the horizon is valid except for situations in which the river has a significant upward slope (these are unusual scenarios in which we do not expect to operate like upstream on a rapid or at a waterfall). In our application domain, the inertial measurement unit on the vehicle would be used to estimate the horizon. Another assumption we make is that the appearance of the above horizon regions is fairly representative of the appearance of the entire shore area in that image.

As a preprocessing step, we first segment out the sky and ignore it during all further computations. To build an online appearance model for discriminating between river and shore regions, we extract two types of patches from the image, those that are part of the shore region and those that are likely to be part of the river. Generating shore patches is trivial, we just sample patches lying above the horizon. We find the patches below the horizon line that are most dissimilar in appearance to those above the horizon and use them as candidate river patches. We then use these patches to train a linear SVM which is then used to classify all parts of the image. Details of each step in the algorithm are given below.

A. Feature Extraction

As described in the Section III, the image is divided into square patches and a feature vector ($X \in \mathbb{R}^n$) is computed for each patch which describes its color, texture and position.

B. Sky Detection

A linear support vector machine trained over a set of labeled images is used to detect the sky in each image. The sky is relatively easy to segment out with a globally trained classifier as its appearance is not as variable as that of the river. Discarding the sky before further processing reduces computation and prevents confusion with shiny, mirror like parts of the water's surface which often appear similar to the sky. Fig. 3(d) shows an example of sky detection. The remainder of the image needs to be classified as either being part of the river or part of the shore.

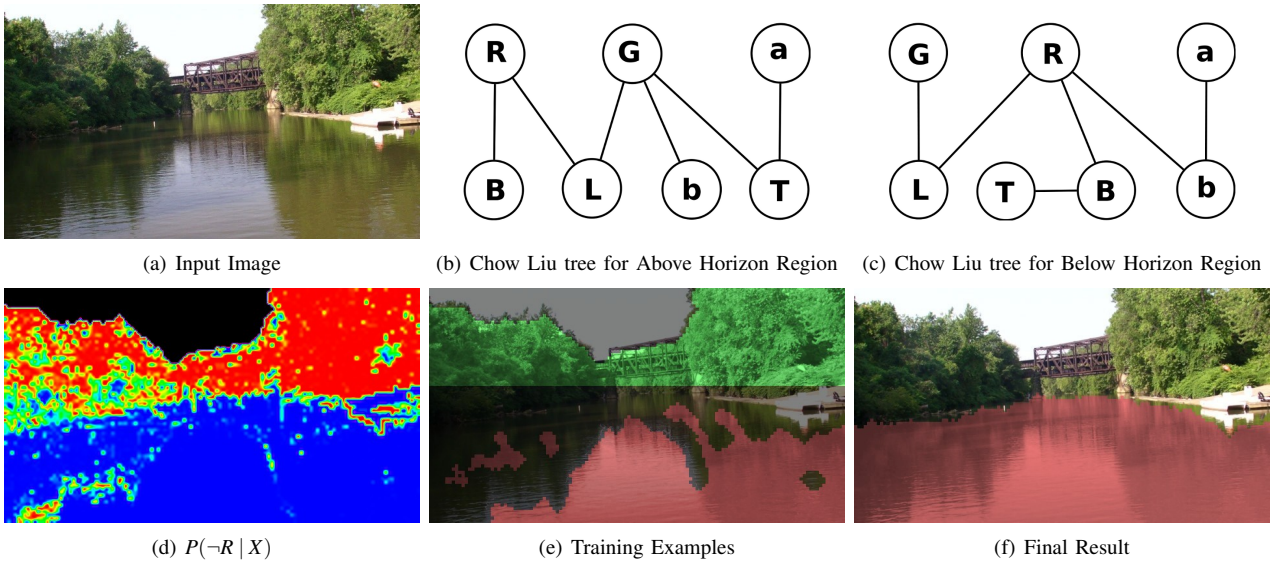

(a) Input Image (b) Chow Liu tree for Above Horizon Region (c) Chow Liu tree for Below Horizon Region

(d) $P(\neg R \mid X)$ (e) Training Examples (f) Final Result

Fig. 3. Steps in the Self-Supervised River Segmentation Algorithm: **(a)** Image input to the algorithm. **(b)** and **(c)** Chow Liu trees built for the above and below horizon parts of the image. In each tree the R, G and B nodes correspond to RGB color features; L, a and b are Lab color feature nodes and T is the texture feature node (norm of the texture descriptor). Edges connect well correlated features, for example above the horizon because of vegetation, the algorithm links greenness of a region (G) to how textured it is (T). **(d)** $P(\neg R \mid X)$: warm colors are used for values closer to 1 (probably shore region). The detected sky region is marked in black **(e)** Training examples: The algorithm finds shore regions (shaded green) and candidate river regions (shaded red) for training a classifier. **(f)** Final result: The classifier is run on the entire image to classify each patch. The detected extent of the river is in red.

C. Appearance Modeling

The goal of the appearance modeler is to assign to each patch a probability of being part of the river (R) or being part of the shore ($\neg R$) on the basis of the feature vector (X) that describes it. By Bayes' Rule we have

$$P(\neg R \mid X) = \frac{P(X \mid \neg R)P(\neg R)}{P(X)} \tag{1}$$

Since the labels (R and $\neg R$) are what we are trying to determine, $P(X \mid \neg R)$ can not be calculated directly. We define a boolean variable H which is true for regions below the horizon and false for regions above. The value of H at each point in the image is known because the horizon is known. We assume that the appearance of the shore region above the horizon is representative of the entire shore region in the image or $P(X \mid \neg R) \approx P(X \mid \neg H)$ which gives

$$P(\neg R \mid X) \approx \frac{P(X \mid \neg H)P(\neg R)}{P(X)} \tag{2}$$

$$= \frac{P(X \mid \neg H)P(\neg R)}{P(X \mid \neg H)P(\neg H) + P(X \mid H)P(H)} \tag{3}$$

$P(\neg H)$ and $P(H)$ are determined from the relative sizes of the above and below horizon regions in the image. $P(\neg R)$ which we arbitrarily set to 0.5 is the prior probability of a patch being part of the shore region. The appearance distributions $P(X \mid \neg H)$ and $P(X \mid H)$ are modeled using Chow Liu trees [12]. A Chow Liu tree is a method for approximating the joint probability distribution of a set of discrete random variables by factorizing it into a product of second order distributions. A Chow Liu tree is optimal in the sense that it is the distribution of its class that minimizes the KL divergence to the real distribution.

The feature vector X contains color, texture and image position information and has high dimensionality as it contains many texture filter responses. It is computationally intractable to use the full length feature vector at this point because of the way Chow Liu modeling scales with dimensionality. Therefore, we use an abridged feature vector $\hat{X} \in \mathbb{R}^d$ in which the texture descriptor subvector is replaced by its L_2 norm. Furthermore, we do not include the image position in $\hat{X}$ because we do not want to model the effect of image position on appearance at this stage.

The features in feature vector $\hat{X}$ are continuous valued while Chow Liu trees work over discrete valued random variables. To solve this problem, each $\hat{X} \in \mathbb{R}^d$ is converted into a discretized feature vector $\tilde{X} \in \mathbb{S}^d$. Each feature in $\tilde{X}$ is assigned to 1 of 16 levels ($\mathbb{S} = \{0,1,2,\ldots,15\}$) using equally sized bins that span the range of values taken by that feature.

Two Chow Liu trees are built, one using the feature vectors of patches above the horizon ($\tilde{X} \notin H$) to model $P(X \mid \neg H)$ and another using the feature vectors of below horizon patches ($\tilde{X} \in H$) to model $P(X \mid H)$. We use subscripts to denote individual features in a feature vector so $\tilde{X}_i$ is the i^{th} feature in feature vector $\tilde{X}$. A Chow Liu tree is a maximal spanning tree of the mutual information graph. The mutual information graph has one node for each feature ($\tilde{X}_i$) and an edge between every pair of nodes ($\tilde{X}_i$ and $\tilde{X}_j$) which is weighted by their mutual information $I(\tilde{X}_i; \tilde{X}_j)$.

$$I(\tilde{X}_i; \tilde{X}_j) = \sum_{x_i=0}^{|\mathbb{S}|-1} \sum_{x_j=0}^{|\mathbb{S}|-1} p(x_i,x_j) \log\left(\frac{p(x_i,x_j)}{p(x_i)p(x_j)}\right) \tag{4}$$

Where $p(x_i)$ is $P(\tilde{X}_i = x_i)$, the probability that the i^{th} feature in $\tilde{X}$ takes on the value x_i and $p(x_i,x_j)$ is the joint probability distribution $P(\tilde{X}_i = x_i, \tilde{X}_j = x_j)$. These distributions are estimated directly from $\tilde{X} \notin H$ and $\tilde{X} \in H$ by counting feature value occurrences and co-occurrences. Edges are pruned from the mutual information graph to form a maximal spanning tree $T = \langle \mathscr{V}, \mathscr{E} \rangle$. The resulting tree encodes the approximate distribution as a product of pairwise conditionals. Figures 3(b) and 3(c) show the Chow Liu trees built for the appearance of above and below horizon regions for a given input image. Each graph contains seven nodes, three each for the RGB and Lab color encodings and one for texturedness. We can calculate $P(\tilde{X} = \tilde{x})$, the probability of occurrence of a particular feature vector $\tilde{x} \in \mathbb{S}^d = \{\tilde{x}_1, \tilde{x}_2, \tilde{x}_3, \ldots, \tilde{x}_d\}$ as follows

$$P(\tilde{X} = \tilde{x}) \approx \prod_{(i,j)\in\mathscr{E}} \frac{p(x_i,x_j)}{p(x_i)p(x_j)} \prod_{j\in\mathscr{V}} p(x_j) \tag{5}$$

The Chow Liu trees for $P(X \mid \neg H)$ and $P(X \mid H)$ are used in (2) to calculate $P(\neg R \mid X)$ for each patch in an image. An example is shown in Fig. 3(d).

D. Classifier Training

For each patch, the probability of being part of the shore region $P(\neg R \mid X)$ is calculated using (2). The patches that are least likely to be on the shore ($P(\neg R \mid X) < \theta$) are used as candidate river patches. Using a low value for θ reduces the chance that shore patches are accidentally used as candidate river patches, but if θ is set too low then the selected region will be too small to provide a good representation of the river region. In our experiments, θ was set to 0.01. The shore patches above the horizon and the candidate river patches with $P(\neg R \mid X) < \theta$ are used to train a two class (river/shore) linear support vector machine.

The SVM uses the unabridged, continuous valued feature vectors X, including image position and the complete texture descriptor. Since we are learning a new classifier for each new frame, while the appearance of the river is likely to remain fairly constant over short periods of time, we initialize the SVM training using the SVM learnt on the previous frame to reduce training time. Fig. 3(e) shows the river and shore training examples selected in an image.

E. Detecting Water

The trained SVM is used to classify all the patches in the image. As a post processing step, small holes in the labeling are filled using morphological operators. An example final segmentation result is shown in Fig 3(f)

V. Results

A. Datasets and Groundtruth

Four datasets were used for evaluating our algorithm. The data collection setup was a tripod mounted camera (a SANYO VPC-CG102BK or Canon SX200IS) placed onboard a small motorboat. The cameras captured 1280×720 images which were downsampled to 640×360. Three of the datasets were collected on the Allegheny river at Washington's Landing in Pittsburgh, PA, U.S.A, the fourth was collected on the Youghiogheny at Perryopolis, PA, U.S.A. The first Allegheny dataset (Allegheny Day) was collected on a summer afternoon, the second (Allegheny Dusk) was collected in the evening and the third (Allegheny Fall) was collected in the afternoon during autumn. The Youghiogheny dataset was collected around noon. Each dataset contains between 120 and 150 images spaced roughly 2 meters apart that were manually segmented for groundtruth information into river, shore (vegetation, structures etc.) and sky regions. An example ground truth labeling is shown in Fig. 4. Also a groundtruth horizon line was marked out on each image.

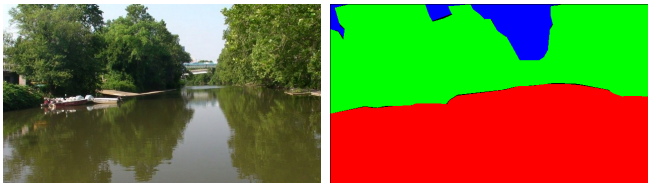

(a) (b)

Fig. 4. **(a)** image from the Allegheny Day dataset **(b)** groundtruth labeling with the river colored red, shore in green and the sky in blue.

The performance metric used is the percentage of pixels misclassified by an algorithm when compared against ground truth. Since the classifiers generate only two output labels and we are not interested in differentiating between the shore and sky we treat them both as a single class (non-river) during performance evaluation. It should be noted that a naïve classifier that marked everything below the horizon as river and everything above the horizon as non-river would have an error rate of around 10% on these datasets.

B. Supervised Segmentation Results

We investigated how well a supervised classifier would be able to generalize to previously unseen environments. From each dataset, 2 images and their groundtruth labelings were picked at random as training examples. Each dataset was classified using two supervised classifiers. The first classifier was trained on the 2 images from the same dataset ('Self' in Table II), the second was a classifier trained on the 6 images from the other 3 datasets('Leave One Out' in Table II). These classifiers were then tested on all the images in the dataset. This process of picking images, training classifiers and testing on all the images was repeated 16 times for each dataset. Table II reports error rates averaged over these 16 trials. It can be seen that the supervised approach worked well when used on datasets it had been trained on but performance often degraded when run on new datasets that were not seen during training. This suggests that a supervised approach does not generalize well to new environments.

TABLE II
Performance of Supervised and Self-Supervised Segmentation Methods: Mean Error(Std dev)

Dataset	Supervised		Our Method
	Self	LOO	
Allegheny Day	3.80% (0.64%)	3.81% (0.63%)	2.75%
Allegheny Dusk	3.10% (0.46%)	9.59% (1.53%)	4.15%
Allegheny Fall	3.05% (0.51%)	10.57% (1.67%)	2.73%
Youghiogheny	3.50% (0.34%)	4.47% (0.41%)	3.22%

C. Self-supervised Segmentation Results

The self-supervised segmentation algorithm described in Section IV was evaluated on the four datasets. Error rates are shown in Table II. Because there is no training step for the self-supervised algorithm, standard deviations are not included with the results. On all four datasets, the self-supervised algorithm outperformed a supervised classifier that was tested on previously unseen datasets. Even when the supervised algorithm was trained on a subset of images from the same dataset it was tested on, it only outperformed the self-supervised method on Allegheny Dusk. This is significant considering how the self-supervised method uses no manually labeled input.

Fig. 5 shows examples of the detected extent of the river along with some intermediate steps of the algorithm. Some failure cases of our algorithm are explained in Fig. 6.

Since the river segmentation is for vehicle guidance, it is important that the algorithm be able to run at around 1 frame per second or faster. Table III shows a profile of the execution time for processing a 640 × 360 image split into 5 × 5 pixel patches with our current MATLAB implementation on an Intel Core2 Q9550 based desktop computer. The execution time indicates that with an optimized C/C++ implementation it should be possible to perform segmentation at 1fps for vehicle guidance.

TABLE III
Algorithm Running Time (MATLAB)

Step	Time taken
Feature Extraction (color)	0.49s
Feature Extraction (texture)	1.08s
Appearance Modeling	0.41s
Classifier Training	0.20s
Final Detection	0.14s
Total	**2.32s**

VI. Conclusions and Future Work

We presented a method for using monocular vision to estimate the extent of a river in an image. We demonstrated that a supervised technique is unlikely to generalize well to different environments. We formulated and evaluated a self-supervised alternative that automatically generates a model of

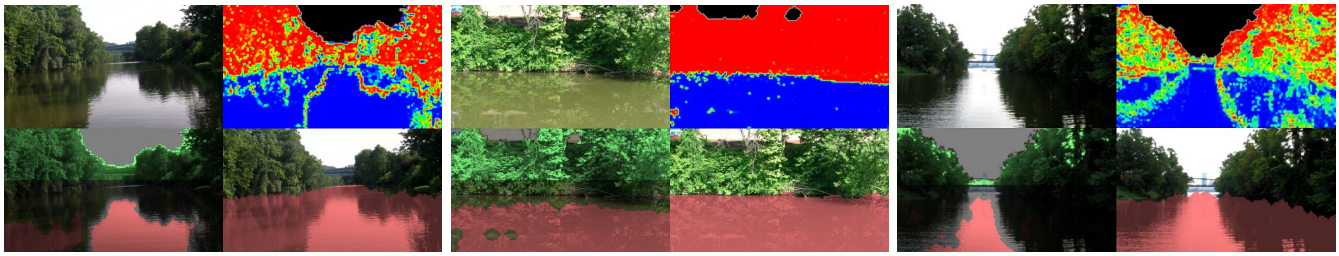

(a) Allegheny Day (b) Allegheny Day (c) Allegheny Dusk

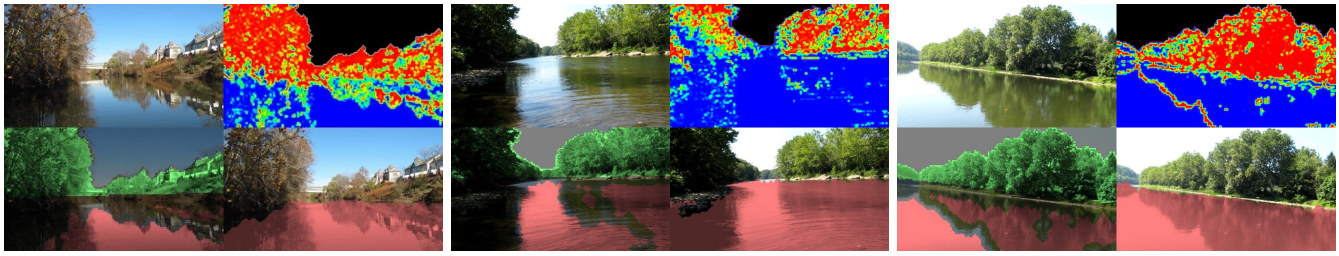

(d) Allegheny Fall (e) Youghiogheny (f) Youghiogheny

Fig. 5. Examples on which the self-supervised method performed well. In each example the top left quadrant is the input, the top right is a heatmap showing the probability of a patch being part of the shore based on its appearance (the detected sky is marked black), the bottom left quadrant shows the automatically detected river and shore regions for training a classifier and the bottom right is the extent of the river as determined by the algorithm.

(a) Allegheny Day (b) Youghiogheny

Fig. 6. Some images on which the self-supervised algorithm failed. In **(a)** the novel objects below the horizon (pier and boat) were misclassified. In **(b)** the grass on the bank is marked as part of the river because a few patches on the bank were picked as river training examples.

river appearance when presented with an image by leveraging assumptions that can be made about the structure of the environment and the horizon.

Our method is completely memoryless and builds a new model for each input image. Using history of previous river appearance to build an adaptive model would provide robustness against failure. The most serious failure mode of our algorithm is when novel objects (like the boats and piers in Fig. 6(a)) appear below the horizon and are misclassified. Our algorithm is unable to handle this because it does not maintain a model of river appearance and because it assumes that the appearance of the above horizon region adequately models all non-river objects. Extending our approach to learn an appearance model from previous images would enable the detection of novel objects below the horizon.

We would also like to investigate the use of priors on likely river shapes and performing inference over multiple frames in a video sequence to increase accuracy.

REFERENCES

[1] A. Saxena, M. Sun, and A. Ng, "Learning 3-d scene structure from a single still image," *IEEE Intl. Conf. on Computer Vision. ICCV*, 2007.

[2] D. Hoiem, A. A. Efros, and M. Hebert, "Automatic photo pop-up," *Proceedings of ACM SIGGRAPH 2005*, 2005.

[3] H. Dahlkamp, A. Kaehler, D. Stavens, S. Thrun, and G. Bradski, "Self-supervised monocular road detection in desert terrain," in *Robotics Science and Systems Conference (RSS'06)*, 2006.

[4] B. Xie, Z. Xiang, H.Pan, and J.Liu, "Polarization-based water hazard detection for autonomous off-road navigation," in *IEEE Intl. Conf. on Intelligent Robots and Systems (IROS'07)*, 2007.

[5] A. Sarwal, J. Nett, and D. Simon, "Detection of small water bodies," in *PrecepTek Robotics Technical Report (ADA433004'04)*, 2004.

[6] H. Kwon, D. Rosario, N. Gupta, M. Thielke, D. Smith, P. Rauss, P. Gillespie, and N. Nasrabadi, "Hyperspectral imaging and obstacle detection for robotics navigation," U.S Army Research Laboratory Technical Report, Tech. Rep. (ARL-TR-3639'05), Sept. 2005.

[7] A. Rankin, L. Matthies, and A. Huertas, "Daytime water detection by fusing multiple cues for autonomous off-road navigation," in *24th Army Science Conference (ASC'04)*, Nov. 2004.

[8] A. Rankin and L. Matthies, "Daytime water detection and localization for unmanned ground vehicle autonomous navigation," in *25th Army Science Conference (ASC'06)*, Nov. 2006.

[9] ——, "Daytime water detection based on color variation," in *IEEE Intl. Conf. on Intelligent Robots and Systems (IROS'10)*, 2010.

[10] K. Laws, "Rapid texture identification," *SPIE*, pp. 376–380, 1980.

[11] E. Tola, V. Lepetit, and P. Fua, "A fast local descriptor for dense matching," in *Conf. on Computer Vision and Pattern Recognition*, 2008.

[12] C. Chow and C. Liu, "Approximating discrete probability distributions with dependence trees," *Information Theory, IEEE Transactions on*, vol. 14, no. 3, pp. 462 – 467, may. 1968.